

Deposition and characterisation of nanostructured silicon-oxide containing diamond-like carbon coatings

V. BURŠÍKOVÁ*, P. DVOŘÁK, L. ZAJÍČKOVÁ, D. FRANTA, J. JANČA, J. BURŠÍK^a, J. SOBOTA^b, P. KLAPETEK^c, O. BLÁHOVÁ^d, V. PEŘINA^e

Faculty of Science, Masaryk University, Kotlářská 2, 61137 Brno, Czech Republic

^a*Institute of Physics of Materials, Academy of Sciences of the Czech Republic, Žitkova 22, 61662 Brno, Czech Republic*

^b*Institute of Scientific Instruments, ASCR, Královopolská 147, 612 64 Brno, Czech Republic*

^c*Czech Metrology Institute Brno, Czech Republic*

^d*West Bohemian University Pilsen, Czech Republic*

^e*Institute of Nuclear Physics ASCR, Rez at Prague, Czech Republic*

Nanostructured diamond-like carbon coatings with various silicon-oxide content were deposited on different substrate materials (silicon, glass, polycarbonate and steel) in capacitively coupled r.f. discharge (13.56 MHz). The structure of the prepared films was studied with infrared absorption spectroscopy (FTIR) and X-ray photoelectron spectroscopy. Complete atomic compositions, including hydrogen content and film densities, were determined by combination of RBS and ERD analyses. The complex dielectric function of the films was determined from ellipsometric measurements in the range 1.5-5.2 eV. Matrix Assisted Laser Desorption-Ionisation – Time of Flight Mass Spectrometry (MALDI-TOF) was used to study the deposited films. The mechanical properties of prepared coatings (e.g. hardness, elastic modulus, fracture toughness, coating/substrate adhesion etc.) were studied by means of depth sensing indentation technique using Fischerscope H100 tester. The tribological properties were studied using CSM pin-on-disc tester. The effect of intrinsic stress on the coating properties was investigated. The variation in SiO_x content enabled to minimize the intrinsic compressive stress in coatings. Analysis of the evolved crack morphology by means of optical microscopy, scanning electron microscopy (SEM) and atomic force microscopy (AFM) revealed a significant increase in interfacial fracture toughness for the DLC:SiO_x films compared to the pure DLC films. On the basis of above described investigation nanocomposite multilayer coatings with enhanced mechanical properties (high hardness, adhesion, fracture toughness, low intrinsic stress) were designed.

(Received August 6, 2007; accepted August 30, 2007)

Keywords: Nanostructured coatings, DLC, Hardness, Adhesion, Fracture toughness

1. Introduction

The amorphous hydrogenated diamond-like carbon (a-C:H, DLC) thin films and their modifications have been of great technological and scientific interest over the past 20 years [1-5]. One of the suitable methods for DLC preparation is the plasma enhanced chemical vapor deposition (PECVD) technique. The PECVD method enables to adjust the film properties and composition by choosing the right deposition parameters and hence make them convenient for a wide variety of applications. In order to obtain DLC structures, the substrates have to be negatively biased relatively to the plasma in order to achieve intensive ion bombardment during the film growth. Increasing ion energy reduces the hydrogen content and tends to generate high intrinsic compressive stresses. The main disadvantages of DLC films prepared using PECVD are their low thermomechanical stability (due to hydrogen loss at temperatures exceeding 300 °C) and high compressive intrinsic stress (due to intense ion bombardment). Various materials derived from DLC have been developed to change and improve their properties. Such materials are similar in structure to DLC but in addition to carbon include nitrogen, silicon and oxygen, fluorine or metal atoms [6-12]. These modifications have

been made to DLC films in order to decrease their high internal compressive stresses, to reduce their surface free energies (e.g. fluorine incorporation), to decrease their already low friction coefficients (silicon-oxide incorporation) or to modify their electrical properties. Nitrogen incorporation has been used to improve field emission properties of DLC films. One particular class of modified DLC coatings are diamond-like nanocomposite films consisting of two amorphous interpenetrating networks, a diamond-like network and a silicon-oxide like network. Due to unique microstructures of these nanocomposite films, they exhibit properties that are different from those of the single component films. The aim of the present work was to develop nanocomposite DLC films with SiO_x content exhibiting enhanced fracture toughness, high surface hardness, low compressive stress and high thermomechanical stability.

2. Experimental

The DLC films with various SiO_x content were prepared in r.f. capacitive discharges at low pressures (8-11 Pa) from a mixture of methane (CH₄) and hexamethyldisiloxane (HMDSO - Si₂OC₆H₁₈). This basic mixture was used either, without any additional gas, or

with an admixture of argon, hydrogen or nitrogen. The reactor was a glass cylinder with two, inner parallel plate electrodes, made of graphite. The bottom electrode, with the diameter of 150 mm, was coupled to the r.f. generator (13.56 MHz) via a blocking capacitor. The substrates (silicon single-crystal, glass, steel, polycarbonate) were placed on the r.f. electrode, the r.f. voltage of which was superimposed with a negative d.c. self-bias. The r.f. power was in the range 50 to 350 W. The corresponding self-bias voltage varied from -250 V to -600 V depending on the gas mixture, applied power and deposition pressure. The CH_4 flow rate was varied in the range from 1.4 sccm to 2.85 sccm. The HMDSO flow rate Q_{HMDSO} varied from 0 to 0.87 sccm. The flow rate of admixed gas (Ar, H_2 or N_2) ranged from 0.35 sccm to 7 sccm.

Excited species and excitation temperature that can approximate the temperature of electrons were studied by optical emission spectroscopy using a Jobin Yvon TRIAX 550 spectrometer. Gas chromatography coupled with mass spectrometry was used for a detection of stable plasma products. The ion saturation current density was measured by means of a capacitively coupled planar probe [13] that helps to get rid of the problem with deposition of an insulating layer common for Langmuir single probes. Within this method the planar probe is r.f. driven by another auxiliary weaker generator working on a different frequency than the discharge itself. By this way the probe is dc negatively biased due to a different mobility of electrons and ions. After switching off the auxiliary generator the probe is being discharged by a saturated ion positive current. This was measured with an oscilloscope several times during the same deposition process showing reproducible values.

The structure of the prepared films was studied with infrared absorption spectroscopy (FTIR) and X-ray photoelectron spectroscopy. Complete atomic compositions, including hydrogen content and film densities, were determined by combination of RBS and ERD analyses. The complex dielectric function of the films has been determined from ellipsometric measurements in the range 1.5-5.2 eV. The surface energy was determined utilizing contact angle measurements using the SEE System.

The depth sensing indentation (DSI) method was used for determination of mechanical properties of the films. In the case of the tester Fischerscope H100 the applied load was registered as a function of indentation depth during loading/unloading cycles. The DSI technique enables to determine the elastic and plastic part of the indentation work (W_e and W_{pl}), the effective elastic modulus ($Y = E/(1-\nu^2)$, where E is the Young's modulus and ν is the Poisson's ratio of the films) and the hardness of the film. In the case of the indentation testing of thin films, the measured properties depend on the indentation depth due to combined response of the coating and the substrate. Therefore, the measured elastic modulus and hardness values were corrected for the substrate influence [14-17]. The morphology of the indentation prints was studied using an optical microscope, a Philips 505 SEM scanning electron microscope and atomic force microscope (AFM).

The so-called critical indentation depth until the first interfacial crack appeared was determined in order to study the resistance of the film-substrate interface against decohesion. The internal stress was determined from measurements of a bending curvature of thin glass strips coated with the studied films.

3. Results and discussion

In the observed emission spectra the most dominant features belong to atomic and molecular hydrogen. Six lines of Balmer series from $\text{H}\alpha$ doublet at 656.285 and 656.273 nm up to $\text{H}\zeta$ at 388.906 nm were detected. The excitation temperature, that approximate the temperature of electrons, was calculated from $\text{H}\gamma$, $\text{H}\delta$ and $\text{H}\epsilon$ lines because here the production of excited states due to hydrogen molecule dissociation can be neglected. Intense atomic and molecular hydrogen emission demonstrates that it is an abundant product of various dissociation reactions of methane or HMDSO. From the fact that atomic emission lines of carbon, silicon or oxygen were not detected at all we can deduce that the dissociation of the molecules is not complete. The emission bands of CH_3 radicals and strong singlet system of CH_2 radicals are unfortunately in UV/VUV range and could not be recorded with our equipment. However, the violet-degraded Q heads at 590.6, 693.2, 695.3, 731.6 and 819.2 nm of the weaker CH_2 triplet system were found. From the CH radical bands only (0,0) band of the ($A^2\Delta-X^2\Pi$) system at 431.4 nm was detected.

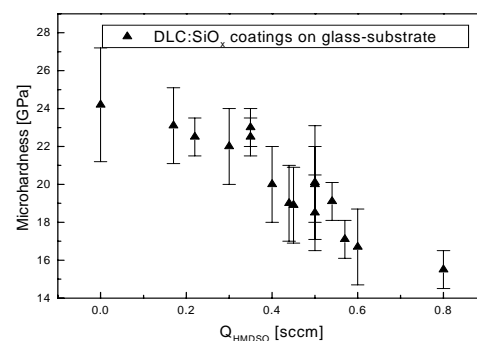


Fig. 1. Film microhardness dependence on HMDSO flow rate. $P=250$ W; methane flow rate $Q_{\text{CH}_4}=1.4$ sccm.

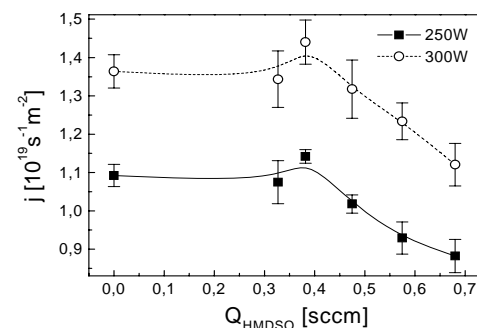
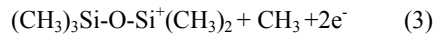
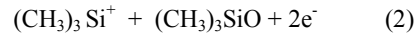
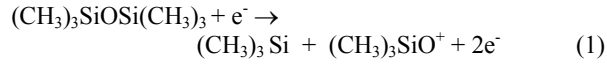
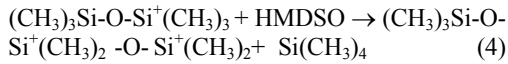


Fig. 2. Dependence of the saturated ion current j on the HMDSO flow rate for two applied powers.

A large number of DLC coatings with various SiO_x content were prepared to find a correlation between the film properties and the discharge conditions for different mixtures. In Fig.1 a dependence of film microhardness on the flow rate of HMDSO (Q_{HMDSO}) is shown. The microhardness was constant in the range of the experimental errors up to 0.4 sccm of HMDSO flow rate and it had decreasing tendency for higher values. A similar dependence on Q_{HMDSO} was observed for the saturated ion current starting from Q_{HMDSO} ≈ 0.4 sccm (see Fig. 2.). Since the saturated ion current is proportional to the positive ion density and inversely proportional to the ion masses it is difficult to separate both effects. However, the decrease in the saturated ion current was related to the oligo/polymer formation in the plasma observed for higher Q_{HMDSO}. Therefore we believe that the increase of ion masses is an important factor. The current density depended linearly on the power. In this case an increase of the density with the power can be main a reason for an increase of the current. Three different types of the dissociative ionization of the HMDSO molecule can occur [18]:



The cation produced by the reaction (3) is a reactive electrophile when compared to oxygen in HMDSO molecule. Therefore it can start an ion oligo/polymerization according to the following reaction:



The product of reaction (4), which was experimentally detected by the gas chromatography, can react in the same way with another HMDSO molecule producing high mass cations. On the other hand, electron attachment and consecutive ion-neutral reactions may lead to the high mass anions. Contrary to the cations the anions are trapped in the plasma and homogeneous reactions finally cause a growth of solid amorphous particles. Indeed, white dust particles were observed in the discharge when Q_{HMDSO} is exceeding 0.4 sccm and the amount of created particles increased with increasing HMDSO flow rate. It is well established that once particles attain a few nm in size they are negatively charged and several forces like electrostatics, ion drag, thermophoresis (gradients in gas temperature), neutral drag (gas flow) and gravity act on them [19]. As a result the particles are confined in the positions where the total net force is zero. This causes clouds of particles to typically resident at the plasma/sheath boundaries. We observed that after the deposition the white macroscopic particles were collected on the glass walls and side parts of the upper electrode where the HMDSO monomer was introduced to the

discharge as well as at the output to the pump. No such particles were observed in the films and therefore we expect they were efficiently repelled from the negatively biased electrode and dragged by the gas flow. This avoided their incorporation into the growing films. Anyway, the production of these particles in the plasma shows that polymeric reactions take place during the deposition and this fact can be related to a significant change not only in the mechanical but also in the optical properties.

The films were investigated by infrared absorption spectroscopy (FTIR), X-ray photoelectron spectroscopy (XPS) and Rutherford backscattering, spectrometry, (RBS) combined with elastic recoil detection analysis (ERDA) in order to assess the film's chemical structure and composition. The bulk concentrations of carbon, hydrogen, silicon and oxygen atoms, composing the DLC:SiO_x films were obtained by RBS and ERDA. The carbon content decreases from 65 to 40 % with increasing HMDSO flow rate while silicon, oxygen and hydrogen increase from 0 to 12 %, from 1 to 3 % and from 35 to 46 %, respectively. It has been already shown that the oxygen-to-silicon ratio was about 0.29, in the range of experimental errors independently on the HMDSO flow rate.

XPS analyses showed that the surface regions of the DLC:SiO_x films (maximum depth of 5 nm) contain more oxygen than the bulk film. In fact, the oxygen-to-silicon ratio decreases from 2.5 in case of the HMDSO flow rate of 0.17 sccm, to about 1.0 for higher HMDSO flow rates, which is still more than three times higher than in the film.

Table 1. Results on critical relative indentation depth (the critical indentation depth-to-film thickness ratio) D_{crit} for various HMDSO flow rates Q_{HMDSO}.

Q _{HMDSO} [sccm]	D _{crit}	Q _{HMDSO} [sccm]	D _{crit}
0	0.16 ± 0.04	0.45	0.91 ± 0.09
0.17	0.57 ± 0.04	0.50	0.74 ± 0.06
0.22	0.88 ± 0.05	0.50	0.61 ± 0.05
0.30	0.84 ± 0.08	0.50	0.51 ± 0.05
0.35	1.17 ± 0.04	0.54	0.41 ± 0.04
0.35	1.12 ± 0.09	0.57	0.38 ± 0.04
0.40	1.14 ± 0.09	0.60	0.27 ± 0.04

In order to obtain comparable fracture characteristics for coatings with different thicknesses we defined the relative critical indentation depth D_{crit} as the critical indentation depth divided by the film thickness. The results for different Q_{HMDSO} are summarized in Table 1. The fracture toughness of the coatings increased with Q_{HMDSO} up to a maximum at about 0.4 sccm and then a decrease mainly because of increasing compressive stress was observed. The AFM image in Fig. 3a shows the initiation of buckling around the indentation print due to a high compressive stress. When the applied load increased the introduced shear stress was high enough to create

delamination of the buckled part (see Fig. 3b). This was detected on the load-penetration curves as a jump. This effect enabled us to determine the depth at which the delamination was created first.

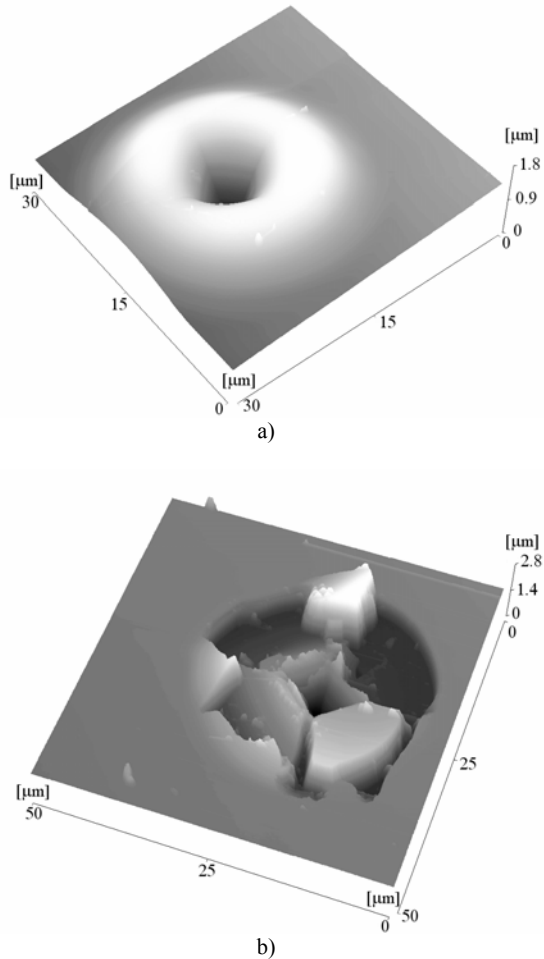


Fig. 3. AFM images of the indentation induced buckling due to high compressive intrinsic stress (a) and the indentation induced delamination around the indentation print.

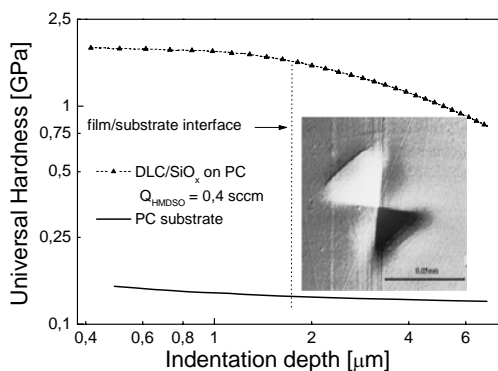


Fig. 4. Universal hardness dependence on the indentation depth of DLC:SiO_x coating on polycarbonate substrate with example of SEM image showing the indentation print made at load of 0.5 N in DLC:SiO_x coating on polycarbonate.

In case of the optimum deposition conditions, $Q_{\text{HMDSO}} = 0.22\text{--}0.45$ sccm, it was possible to prepare coatings with a high thermomechanical stability. Within this flow rate region the effective elastic modulus of the films was 120 ± 5 GPa that is lower compared with the pure DLC elastic modulus of 160 ± 5 GPa. With increasing Q_{HMDSO} the effective elastic modulus had further decreasing tendency. With aim to increase the adhesion of the deposited films to the substrates the plasma treatment in hydrogen discharge was carried out before the deposition. This had a significant effect especially for the polycarbonate and the high fracture resistance of this type of coating/substrate system is illustrated by depth dependence of the universal hardness and a SEM image in Fig. 4. In case of the films deposited at optimum deposition conditions on the plasma treated polycarbonate the indenter was in the depth of 10 μm , when the first film fracture appeared. This depth almost seventimes exceeded the film thickness showing the extremely high indentation resistance due to increased interfacial strength and low internal stress in the films. In the case of the pure DLC films without a HMDSO addition or films prepared from pure HMDSO the spontaneous delamination and fracture were observed (Fig. 5).

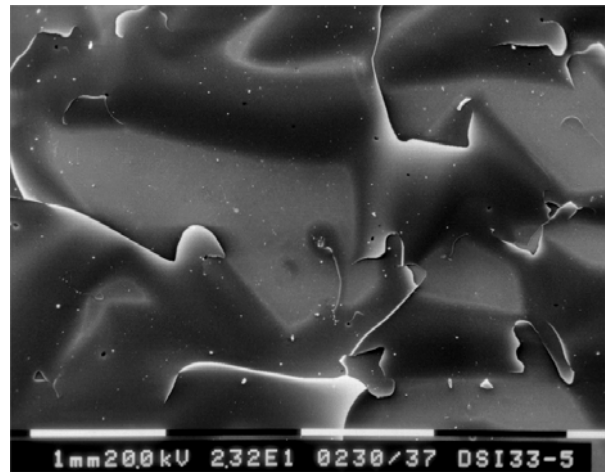


Fig. 5. SEM micrograph of the completely delaminated coating, prepared from pure HMDSO. The film thickness was 0.7 μm . The same effect was observed for pure DLC coating, thicker than 0.3 μm .

The tribological properties of the nanostructured silicon-oxide containing DLC films deposited on glass substrate were studied using CSM pin-on-disc tester. The wear resistance and friction properties were studied by Al₂O₃ ball using testing loads in the range from 5 to 15 N. The obtained friction coefficient was in the range from 0.04 to 0.08 for coatings with optimum conditions.

4. Conclusions

We have deposited DLC:SiO_x films with different amounts of silicoxide. The films were mainly composed

of C-C, C-H and C-Si bonds. No C-O bonds were detected in the films. The concentration of silicon and oxygen increased with increasing HMDSO flow rate. The film surfaces were richer in oxygen and consequently the Si-O and C-O bonds were observed by XPS. The film hardness, elastic modulus, interfacial fracture toughness was studied in dependence on silicon and oxygen concentration. It was found that the incorporation of silicon and oxygen (SiO_x) into the DLC network significantly increased the interfacial fracture toughness and decreased the compressive stress in the films compared to pure DLC coatings. We have determined the optimum silicon and oxygen percentage in the DLC network at which the thermo-mechanical stability of the DLC films was improved, whilst keeping the useful DLC properties.

Acknowledgement

This work has been supported by the Science Foundation of the Czech Republic, contracts 106/05/0274 and 202/05/0607 and by Ministry of Education, Youth and Sports of the Czech Republic, contracts MSM 0021622411 and 1K05025. The authors are grateful to Dr J. Houdkova and Dr J. Zemek from the Institute of Physics ASCR for XPS measurements.

References

- [1] A. Grill, B. Meyerson, *Synthetic Diamond: Emerging CVD Science and Technology*, Ed: K. E. Spear, J. P. Dismukes, Wiley, NewYork, 91 (1994).
- [2] A. Grill, *Surf. Coat. Technol.* **94-95**, 507 (1997).
- [3] Dj. M. Maric, P. F. Meier, S. K. Estreicher, *Mater. Sci. Forum* **83-87**, 119 (1992).
- [4] M. A. Green, *High Efficiency Silicon Solar Cells*, Trans Tech Publications, Switzerland (1987).
- [5] L. Martinu, *Plasma Processing of Polymers*, Kluwer Academic Publisher, NATO ASI Series E: **346**, 247 (1996).
- [6] M. Grishke, A. Hieke, F. Morgenweck, H. Dimigen, *Diamond. Rel. Mater.* **6**, 559 (1997).
- [7] C. De Martino, G. Fusco, G. Mina, A. Tagliaferro, L. Vanzetti, L. Calliari, M. Anderle *Diamond. Rel. Mater.* **6**, 559 (1997).
- [8] S. S. Camargo Jr., R. A. Santos, A. L. Baia Neto, R. Carius, F. Finger, *Thin Solid Films* **332**, 130 (1998).
- [9] J. C. Damasceno, S. S. Camargo, M. Cremona, *Thin Solid Films* **420-421**, 195 (2002).
- [10] V. Buršíková, V. Navrátil, L. Zajíčková, J. Janča, *Mater. Sci. Eng.* **A324**, 251 (2001).
- [11] D. Franta, I. Ohlídal, V. Buršíková, L. Zajíčková: *Diamond Rel. Mater.* **12**, 1532 (2003).
- [12] L. Zajíčková, V. Buršíková, V. Peřina, A. Macková, J. Janča, *Surface and Coating Technology* **174 – 175**, 281 (2003).
- [13] N. St. J. Braithwaite, J. P. Booth, G. Gunge, *Plasma Sources Sci. Technol.* **5**, 667 (1996).
- [14] W. C. Oliver, G. M. Pharr, *J. Mater. Res.* **7(6)**, 1564 (1992).
- [15] M. T. Kim, *Thin Solid Films* **283**, 667 (1996).
- [16] M. F. Doerner, W. D. Nix, *J. Mater. Res.* **1**, 6501 (1986).
- [17] I. J. Ford, *Thin Solid Films* **245**, 122 (1994).
- [18] M. R. Alexander, F. R. Jones, R. D. Short, *J. Phys. Chem.* **B101(18)**, 3614 (1997).
- [19] J. Perrin, P. Molinas-Mata, P. Belenguer, *J. Phys. D Appl. Phys.* **27**, 2499 (1994).
- [20] D. Franta, I. Ohlídal, V. Buršíková, L. Zajíčková, *Thin Solid Films* **455-456(1)**, 393 (2003).
- [21] B. Dischler, A. Bubenzer, P. Koidl, *Solid State Communications* **48(2)**, 105 (1983).
- [22] G. Herzberg, *Infrared and Raman spectra of polyatomic molecules*, Van Nostrand, Princeton N.J., (1945).
- [23] S. F. Durrant, R. P. Mota, M. A. Bica de Moraes, *Vacuum*, **47(2)**, 187 (1996).
- [24] K. Aumaille, C. Vallee, A. Granier, A. Gouillet, F. Gaboriau, G. Turban, *Thin Solid Films* **359**, 188 (2000).
- [25] M. Horák, D. Papoušek, *Infrared Spectra and Molecular Structure*, Academia, Praha, (1976).
- [26] N. Fourches, G. Turban, B. Grolleau, *Appl. Surf. Sci.* **68**, 149 (1993).
- [27] J. Malzbender, G. de With, J. M. J. den Toonder, *Thin Solid Films* **366**, 139 (2000).

*Corresponding author: vilmab@physics.muni.cz